HAL open science

Potential benefits of radial secondary injection of helium in dual-bell nozzles

Brian Legros, Luc Léger, Amer Chpoun, Mohamed Sellam, Azeddine Kourta

To cite this version:

Brian Legros, Luc Léger, Amer Chpoun, Mohamed Sellam, Azeddine Kourta. Potential benefits of radial secondary injection of helium in dual-bell nozzles. 57th 3AF International Conference on Applied Aerodynamics, 3AF, Mar 2023, Bordeaux, France. hal-04386970

HAL Id: hal-04386970

https://hal.science/hal-04386970

Submitted on 11 Jan 2024

HAL is a multi-disciplinary open access archive for the deposit and dissemination of scientific research documents, whether they are published or not. The documents may come from teaching and research institutions in France or abroad, or from public or private research centers.

L'archive ouverte pluridisciplinaire **HAL**, est destinée au dépôt et à la diffusion de documents scientifiques de niveau recherche, publiés ou non, émanant des établissements d'enseignement et de recherche français ou étrangers, des laboratoires publics ou privés.

57th 3AF International Conference
on Applied Aerodynamics
29 — 31 March 2023, Bordeaux – France

AERO2023-9-LEGROS

Potential benefits of radial secondary injection of helium in dual-bell nozzles

Brian Legros[1,3], Luc Léger[1], Amer Chpoun[2], Mohamed Sellam[2] and Azeddine Kourta[3]
[1] *National Centre for Scientific Research CNRS – Institute ICARE,*
1C Av. de la Recherche Scientifique, 45100 Orléans, France, brian.legros@cnrs-orleans.fr
[2] *LMEE, Université Paris Saclay-Evry, 40, rue du Pelvoux, CE1455*
[3] *University of Orléans, INSA-CVL, PRISME, 8 Rue Léonard de Vinci,*
45100 Orléans, France, azeddine.kourta@univ-orleans.fr

ABSTRACT

Radial secondary injection of air in the extension section of dual-bell nozzles (DBN) have been the subject of recent studies. The technique showed promise in solving the early transition problem in DBNs, but also in reducing the side-loads generated during the transition phases. Because helium is used to pressurise rocket launcher's fuel tanks, the idea of using radial secondary injection of helium in the extension section of a DBN became of interest. This paper compares the impact of a radial secondary injection of helium in a DBN to a parametrical investigation performed with secondary injection of air. It was found that the use of helium resulted in a transition nozzle pressure ratio (NPR) and a retransition NPR increase of 5.5% and 11.4% respectively compared to test cases using secondary injection of air with a similar secondary pressure ratio. The lateral forces generated by the nozzle during the transition and the retransition phases were brought below 1% of the nozzle thrust by using helium or air as injectant gas. Moreover, the use of helium suppressed the hysteresis effect by causing an identical specific impulse curve trajectory during the transition phases and the retransition phases. Finally, the thrust jumps during transitions and retransitions were dramatically decreased, particularly with the use of helium, suggesting the promising potential of DBN on rocket launchers.

1. INTRODUCTION

The ever-increasing number of satellites to be launched into space have triggered numerous companies to emerge in order to get a market share. The rising number of competitors have pushed companies and state agencies to decrease their launching cost and to increase their launchers' efficiency to remain competitive. Launchers such as Ariane 5 use parallel staging which requires the first stage engine to be ignited before the lift off for reliability reasons [1]. Therefore, the first stage engine is doomed to suffer from off-design operating conditions during the launcher's ascent, which induces high losses. Since the nozzle geometry is designed for a specified performance and the ambient pressure decreases during the launcher's ascent, the nozzle experiences different flow conditions: overexpansion, adapted flow and underexpansion (see Fig. 1). To prevent flow separation inside rocket nozzles at low altitudes (see Fig. 1) and therefore avoid flow instabilities and unsteady side-loads, the nozzle exit area is reduced, even though it implies lower performances at high altitudes.

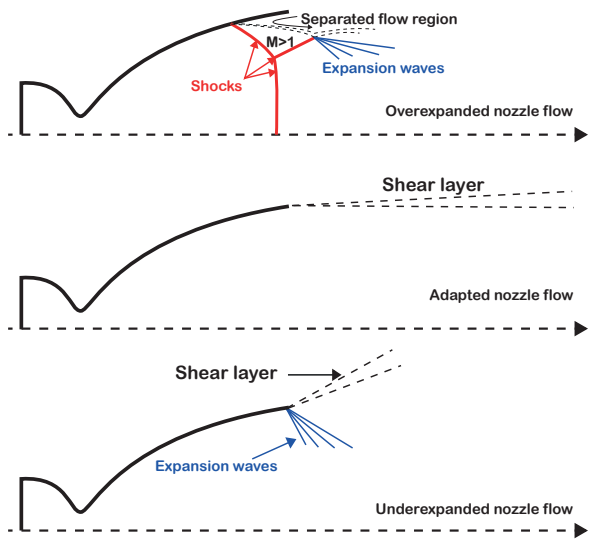

Figure 1: Conventional bell nozzle working modes.

Ideally, the perfect nozzle should be able to increase its exit area during the launcher's ascent in order to adapt to the ambient pressure variations. Nevertheless, this solution would dramatically increase the complexity of the nozzle and decrease its reliability. Many nozzle concepts with altitude adaptive capabilities have been investigated in the past, yet this paper deals solely with the dual-bell nozzle concept. The dual-bell nozzle (DBN) concept was first mentioned by Swan [2] and consists of a converging/diverging nozzle, where the diverging section is com-

posed by two successive nozzle profiles of different expansion ratios. The first part of the divergent, called the base nozzle, provides better performances at low altitudes with little risks of side-loads. The second part of the divergent, called the extension nozzle, provides better performances at high altitudes. The DBN geometry used in the present paper is illustrated in Fig. 2.

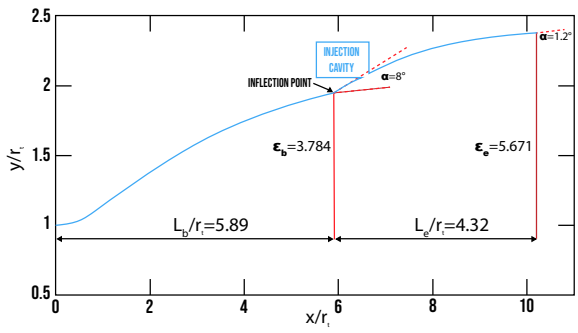

Figure 2: Geometrical parameters of the DBN profile used during the test campaign.

The base nozzle and the extension nozzle are linked together through an inflection region. In sea-level mode, the flow detaches from the nozzle wall at the inflection point, providing a controlled and symmetric separation, therefore limiting the generation of lateral forces. As the launcher ascends in the atmosphere and the ambient pressure decreases, the flow will suddenly reattach the nozzle extension wall, moving the separation location at the nozzle exit. The attached flow in the entirety of the nozzle will provide a higher nozzle pressure ratio and therefore better performances in high altitudes. Fig. 3 shows schlieren images of the DBN in low-altitude mode and high-altitude mode during an experiment performed in the wind tunnel described in Sec. 2. In low-altitude mode, due to the high ambient pressure, the flow separates at the inflection point, which is the onset of the separation shock location (1). The separation shock propagates downstream until being reflected on the nozzle symmetry axis. The reflected shock (3) is then reflected on the exhaust plume boundary (2) further downstream. This process continues to form a succession of compression and expansion cells. In high-altitude mode, the flow is attached to the extension nozzle wall and the DBN is said to be full flowing. In this case, an expansion fan (5) is present at the inflection point. In Fig. 3, because the DBN extension profile geometry is characterised by a constant wall pressure, an internal recompression shock (6) emerges from the inflection point and directly interacts with the nozzle lip shock (7). The nozzle lip shock intersects with a Mach disc (8) at the triple point further downstream (see Fig. 3). The reflected shock (3) issued from the triple point is then reflected on the exhaust jet boundary (2). This process also continues downstream, forming a succession of compression and expansion cells.

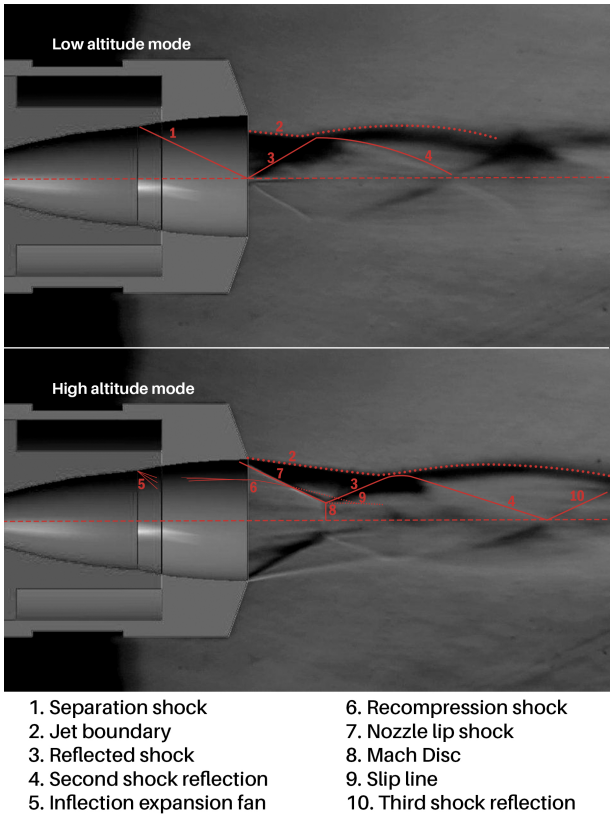

Figure 3: DBN in low-altitude mode (NPR = 15) on the top and high-altitude mode (NPR = 20) on the bottom.

The promising potential of dual-bell nozzles to reduce the cost of access to space fuelled an increasing number of investigations in many research centers [3, 4, 5, 6]. Optimisation codes developed to quantify the financial gain on an Ariane-5-like launcher mounted with a dual-bell nozzle revealed a significant payload mass gain into geostationary transfer orbit of 490 kg [1]. Recent analysis performed in [7] for similar operating conditions indicated a payload mass gain of 1.5 tons using a DBN equipped with an optimised radial secondary injection in order to control the transition. The DBN appears to be a promising and easy-to-implement concept, with no cooling problems. However, three main issues have to be mindfully considered to make the DBN a viable concept: 1) Early transition and retransition, 2) Side forces generation, 3) Stability. Ideally, the transition from low-altitude mode to high-altitude mode (and vice versa) must take place as close as possible to the optimum transition point (see Fig. 4) to provide the best performances. However, the natural transition and retransition in DBNs occur before the optimum transition point (as seen Fig. 4), causing the loss in specific impulse. Consequently, an efficient and reliable method has to be implemented to delay these critical phases. Besides, the shift from one

mode to the other triggers dangerous side-loads caused by unsteady and asymmetrical flow separation in the extension section, which could be detrimental to the rocket integrity [8, 9]. The transition process in DBNs depends on several parameters that are still the subject of numerous studies: Reynolds Number and temperature, testing environment, nozzle geometry, ambient pressure fluctuations, etc. [9, 10, 11, 12, 13].

The extension nozzle profile type in DBNs is among the most important parameters in regard to the transition behaviour [14]. There are three different types of extension profiles: Negative wall Pressure gradient (NP), Positive wall Pressure gradient (PP), and Constant wall Pressure (CP). It was shown in [15] that the separation location depends on the nozzle pressure ratio in NP extension profiles and was well predicted by flow separation criteria such as the Schmucker's criterion. However, the progressive movement of the separation front is the cause of important side-loads [4, 15]. In the case of PP extension profiles and CP extension profiles, a sudden transition is observed experimentally [4, 15] and numerically [16]. The sudden movement of the separation front in the extension reduces the risks of side-loads generation during the transition and the retransition phases [4, 15, 17]. The extension length also plays an important role in DBNs as a shorter extension would decrease the lever arm, and consequently reduce the side-loads moment. However, a decrease in extension length reduces the hysteresis effect (difference between the transition NPR and the retransition NPR) of the DBN and therefore its stability [9]. Numerous studies showed that DBNs were sensitive to the testing environment, namely whether the tests were performed in altitude chambers or at ambient conditions. The variation of the feeding total pressure to increase (resp. decrease) the nozzle pressure ratio during experiments significantly influences the behaviour of DBNs. It changes the Reynolds number during the experiment and modifies the effective wall shape of the inflection region [10, 14, 18, 19, 20].

Even though many of the previous studies brought to light important information regarding DBNs behaviour during the ascent and the descent phases, few have focused on the control of transition and retransition in DBNs. Flow control in rocket nozzles has been the subject of previous studies, whether to prevent flow separation in overexpanded nozzles, to control thrust vector, or to decrease side-loads amplitude on a launching pad [21, 22]. Flow control in dual-bell nozzles has been mainly investigated by using film cooling and secondary injection normal to the mainstream direction, principally to control the transition.

Investigations on film cooling in the vicinity of the inflection region showed a decrease in transition NPR in [23], but an increase of it for Proshchanka et al. in [24]. A decrease in thrust jump (an example of thrust jump is shown in Fig. 4) during the transition phases, and lower lateral forces were also reported. In [25], Martelli et al. showed an effective capability of lowering the wall temperature at the cost of long-lasting lateral forces capable of exciting a nozzle structural mode.

The use of radial secondary injection showed that outstanding gains could be found even for relatively small secondary mass flow rates. A radial secondary injection of air behind the inflection region significantly increased the transition NPR and the retransition NPR [26]. The secondary fluid acts as an obstacle to the upstream flow, triggering a forced and symmetrical flow separation in the vicinity of the inflection region. Using the radial secondary injection, the flow will remain detached on a longer NPR range and bring one towards the optimum transition point [11, 26]. Furthermore, Léger et al. [27] showed that radial secondary injection impacts the nozzle stability and it reduces side-loads generation. It was also found that secondary injection reduced the flip-flopping behaviour of the shock system during the retransition phases, where the flip-flopping phenomenon corresponds to a high amplitude and unsteady displacement of the separation point.

In this paper, the authors study the potential benefits of helium radial secondary injection in a dual-bell nozzle compared to the secondary injection of air.

2. EXPERIMENTAL SETUP

The experiments were performed in the EDITH depressurized wind tunnel (WT) (see Fig. 5), the same test facility as described in [27]. EDITH is one of the rare nozzle testing facility in Europe offering nozzle exit pressure variations. Dry air from 320 litre tanks and pressurised at 300 bar is regulated to 3.5 bar to generate the DBN feeding total pressure in the stagnation chamber. The air from the stagnation chamber travels through the dual-bell nozzle and exits in the depressurised WT test section. The pressure inside the test section is controlled by a valve located in the WT diffuser, upstream of an overall 345 kW pumping group. The control of the position of the valve allows the decrease and the increase of pressure inside the WT test section. During the experiments, the dual-bell nozzle is mounted on a force balance designed by the authors and which moves freely along the (x,y,z) orthogonal axis. The thrust and lateral forces are measured by the force balance using four HBM S2 strain-gauge force transducers, whose signals are amplified to a 0-10 V range before being acquired by the SCXI-1140 cards, at the rate of 1 kHz. The HBM S2 is a force sensor with an accuracy class of 0.05 which provides high accuracy measurements with a sensitivity of 2mv/V. Two transducers of 200 N located on both sides of the force balance were used to measure the vertical force component; one 200 N transducer measured the nozzle thrust; and a 20

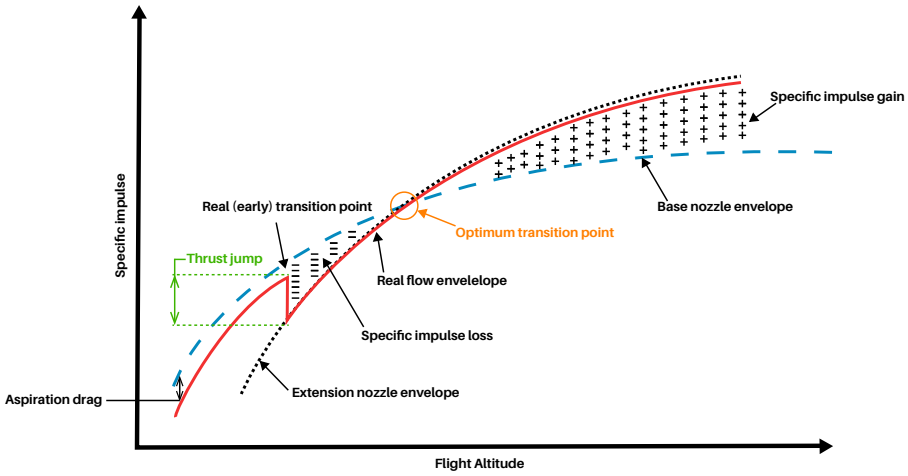

Figure 4: DBN efficiency compared to conventional nozzles.

N transducer measured the lateral forces. Previous studies for the validation of the force balance measurements showed a 0.24 N standard deviation for the force measurements on the longitudinal axis, 0.06 N on the vertical axis and 0.17 N on the lateral axis.

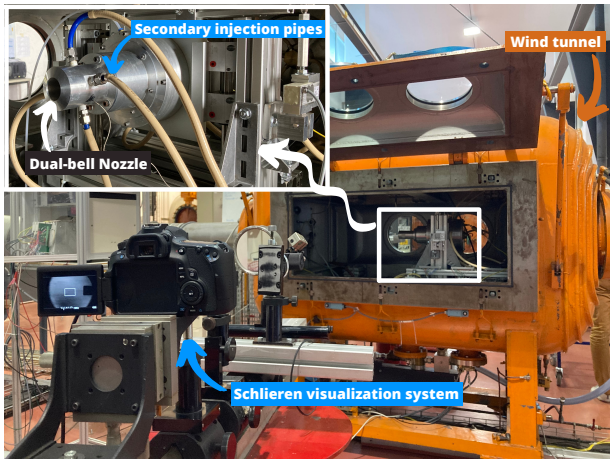

Figure 5: EDITH wind tunnel testing facility.

The base nozzle was designed as a truncated ideal contour (TIC) for an exit Mach number of 3.2, and the extension nozzle was built as a constant pressure (CP) extension profile. To actively control the flow transition and retransition behaviour, a secondary flow of helium or air was radially injected in the extension part of the DBN. The 0.2 mm width injection slot was made possible by manufacturing the DBN in two parts, and the slot was placed 8 mm downstream of the inflection point. This technique also allowed the creation of a settling chamber for the secondary injection (called cavity, and visible in Fig. 6), to provide an axisymmetric, homogeneous secondary injection.

In this study, a test campaign has been carried out to

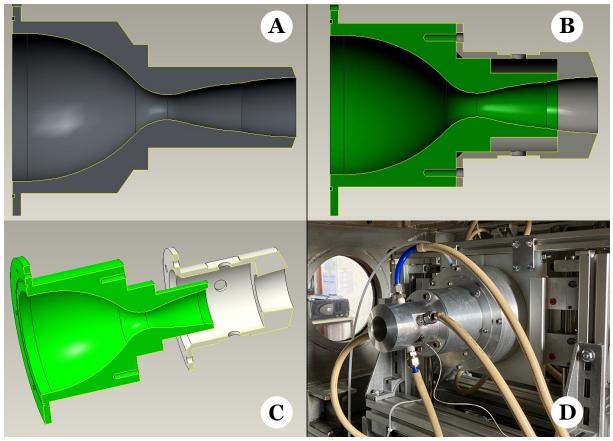

Figure 6: A) DBN without secondary injection (smooth DBN), B) DBN used for experiments with secondary injection, C) Exploded view of the DBN used for experiments with secondary injection, D) DBN mounted with secondary injection pipes in the EDITH wind tunnel.

compare the influence of air and helium as injectant gas on the DBN transition behaviour. In this case, several secondary injection pressures were used for air, ranging from 0.37 bar to 2.17 bar. Only one secondary injection pressure was used for helium: 0.31 bar. For all experiments, the DBN feeding total pressure was kept constant at 3.5 bar and the ambient pressure was varied using the main exit valve located upstream of the pumping group to trigger the transitions and the retransitions in the DBN. When secondary injection was used, the injection pressure was kept constant throughout the experiment. The ambient pressure and the secondary feeding total pressure inside the cavity were measured using Kulite XCQ-062 pressure transducers of 0-100 kPa range. For secondary injection pressures above 90kPa, the pressure transducer inside the cavity was replaced by a Kulite XCQ-093 of 0-350 kPa

with a sensitivity of 28.743 mV/bar. Geometrical details of the DBN profile obtained by an in-house code based on the method of characteristics are presented in Fig. 2, and the reader can find further details in [27,28].

3. RESULTS AND DISCUSSIONS

3.1 Helium and air secondary injection effects on dual-bell nozzle behaviour

This section exposes the impact of air and helium as secondary injectant gas on a dual-bell nozzle transition behaviour. The study compares the results obtained using one secondary injection pressure for helium to several injection pressures for air. During each experiment, the feeding total pressure was kept constant and the ambient pressure in the wind tunnel was repetitively increased and decreased to trigger the transitions and the retransitions inside the DBN. For each experiment, the chosen secondary injection pressure was kept constant. Several secondary injection pressures were considered. The secondary pressure values (P_i), the secondary pressure ratios (SPR=P_i/P_0), the theoretical secondary mass flow rates ($\dot{m}_i$) and the secondary mass flow rate ratios ($\varphi_{\dot{m}} = \dot{m}_i/\dot{m}$) are detailed in Tab. 1. Here, $\dot{m}$ corresponds to the mainstream, theoretical mass flow rate of 0.187 kg/s. Fig. 7 shows the evolution of the measured parameters during a typical experiment using a constant air SPR of 0.15.

At SPR = 0.15 and below NPR = 17.76, the dual-bell nozzle is in the low-altitude mode, where the flow detaches from the wall in the vicinity of the inflection region. When the NPR (red curve in Fig. 7) is increased from its lowest values, the specific impulse generated by the nozzle increases until a sudden drop in specific impulse occurs at NPR = 17.77. At NPR = 17.77, the transition takes place and the flow reattaches the extension wall. During this phase, the DBN switches from the low-altitude mode, to the high-altitude mode. Reciprocally, decreasing the NPR from the high-altitude mode will eventually trigger the retransition process, switching the DBN working mode from high-altitude, to low-altitude. Previous studies on the present DBN revealed important side-loads peaks during transition and retransition phases ([11, 26, 27]), however, Fig. 7 shows that side-loads generation can be mostly suppressed with the use of radial secondary injection, as the peaks are hardly identifiable.

Instantaneous data during a transition and a retransition for several SPR cases are displayed in Fig. 8 and Fig. 9. Both figures display, on top, the specific impulse as a function of nozzle pressure ratio for the DBN without injection slot (called smooth DBN and visible in Fig. 6), the DBN with two secondary injection of air and one secondary injection of helium. On the bottom, Fig. 8 and Fig. 9 show the side-loads-to-thrust ratio. The instantaneous data measurements revealed that, not only the use of secondary injection of air delays the transition NPR (NPR_{trans}) and the retransition NPR ($NPR_{retrans}$), but it also reduces the side-loads generated during the transition from one mode to the other. As shown in Fig. 8, for SPR = 0.15, the side-loads peaks could not be identified as the signal falls within the measurements noise. The use of secondary injection of helium significantly delays the NPR_{trans} and the side-loads peaks fall within the measurement noise. During the descent phases, the use of secondary injection of air and helium increases the $NPR_{retrans}$ and outstandingly reduces the lateral forces generated (see Fig. 9). The evidence of the previously described behaviour is investigated in more details below with averaged data measurements with their standard deviation.

Fig. 10 shows the evolution of the NPR_{trans} and $NPR_{retrans}$ as a function of SPR. The configuration associated with a SPR of 0 on Fig. 10, Fig. 12 and Fig. 13, corresponds to the case with DBN with secondary injection slot but without any injection. The experiments performed with radial secondary injection in the extension profile confirm that the NPR_{trans} and the $NPR_{retrans}$ are greatly influenced by the SPR and the properties of the injectant gas (see Fig. 10). The use of air as injectant gas revealed an increase in NPR_{trans} when the SPR was increased. The maximum NPR_{trans} reached 18.39 and was achieved at SPR = 0.25, corresponding to an increase of 15.5% compared to the SPR = 0 case and an increase of 23.9% compared to the smooth nozzle configuration. Further increase in SPR showed a decrease in NPR_{trans}. The largest decrease in NPR_{trans} following the maximum value achieved was reached at SPR = 0.62 and amounted to 5.7%, bringing down the NPR_{trans} to 17.34. A similar behaviour was identified for the retransition process, as the $NPR_{retrans}$ increased with an increase in SPR up to SPR = 0.36. The maximum $NPR_{retrans}$ reached 17.45, corresponding to an increase of 17.8% and 20.1% compared to the SPR = 0 case and smooth case, respectively. Similarly, further increase in SPR showed a decrease in $NPR_{retrans}$. The largest decrease in $NPR_{retrans}$ following the maximum value achieved was reached at SPR = 0.62 and amounted to 0.9%, bringing down the $NPR_{retrans}$ to 17.29. Fig. 10 shows that delaying the NPR_{trans} and the $NPR_{retrans}$ is limited as there exists a SPR from which an increase in secondary injection pressure causes a decrease in NPR_{trans} and $NPR_{retrans}$. High SPR might change the physics involved in the flow and further investigations using CFD should provide explanations to the previous phenomenon. In the helium configuration, only one secondary pressure ratio was considered: SPR = 0.09. It was found that the NPR_{trans} and the $NPR_{retrans}$ were further increased compared to the results obtained with air for a similar SPR. Compared to the air SPR = 0.11 configuration, the experiments per-

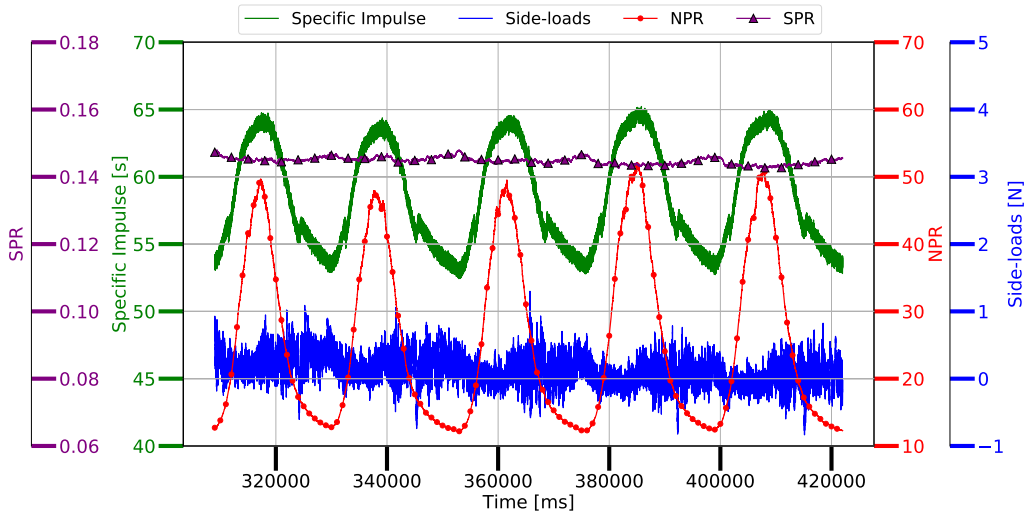

Figure 7: Evolution of the specific impulse, nozzle pressure ratio (NPR), side-loads, and secondary pressure ratio (SPR) as a function of time during an experiment of DBN with an air SPR = 0.15.

Table 1: Secondary injection pressure, pressure ratio, mass flow, and mass flow ratio used in the test campaign.

P_i [bar]	0.37	0.51	0.69	0.88	1.26	1.63	2.17	0.31 (Helium)
SPR	0.11	0.15	0.2	0.25	0.36	0.47	0.62	0.09
$\dot{m}_i$ [g/s]	1.98	2.73	3.7	4.72	6.73	8.75	11.63	4.79
$\varphi_{\dot{m}}$	0.011	0.015	0.02	0.025	0.036	0.047	0.062	0.026

formed with helium revealed an increase in NPR_{trans} and $NPR_{retrans}$ of 5.5% and 11.4% respectively. The NPR_{trans} and the $NPR_{retrans}$ reached 18.19 and 18.68 respectively. However, in this case, the NPR_{trans} was less than the $NPR_{retrans}$. The previous remark does not imply that the hysteresis effect is reversed, it indicates that the hysteresis effect is suppressed. Fig. 11 shows the specific impulse as a function of NPR for a configuration using air and a configuration using helium during a transition and a retransition phase. It shows that the specific impulse trajectory during the transition phase is relatively close to the specific impulse trajectory during the retransition phase in the helium configuration compared the configuration using air. Because the NPR_{trans} (resp. $NPR_{retrans}$) is taken when the specific impulse jump takes place during increasing (resp. descending) NPR phases, the superimposed curves imply higher $NPR_{retrans}$ than NPR_{trans}. It is worth mentioning that the secondary injection of helium and air for SPR = 0.11 were not made at sonic speed due to the low feeding injection pressure. Further experiments using higher SPR for the helium configuration might lead to a better understanding of the aforementioned phenomenon.

Regarding the air configuration, the hysteresis was the largest for the SPR = 0 configuration, reaching 7%, then decreased to 2.7% for SPR = 0.11, and progressively increased along with the secondary injection pressure to hit a maximum of 5.7% for SPR = 0.2. A further increase in SPR induced a decrease in stability as the hysteresis became smaller, dropping to 0.3% for the highest SPR. The influence of the subsonic jet at SPR = 0.11 may have played a role in the early retransition in this specific case, as the cavity is free to suck or blow air freely in the vicinity of the injection slot region.

Fig. 12 shows that the side forces were reduced by using radial secondary injection in both configuration: air and helium. At SPR = 0.09 for helium and for SPR = 0.15 and above for air, the side-loads generated during the transitions and the retransitions fall within the balance measurement noise ($\pm$ 0.5 N) and the force balance could not measure any side-load peaks. At SPR = 0.09 for helium and at SPR $\geq$ 0.11 for air, the side-loads during transition dropped below 1% of the nozzle thrust, against 2.4% of the nozzle thrust in the smooth DBN case. Secondary injection of air brought side-loads during retransition below 1% of the nozzle thrust for SPR = 0.15 and above, against 3.4% in the smooth DBN configuration, providing over three times lower lateral forces magnitude compared to the smooth nozzle configuration. Secondary injection of helium at SPR = 0.09 also brought side-loads generation during retransition phases below 1% of the nozzle thrust. From SPR = 0.36 and above, a slight increase in lateral forces is visible during both, transition and retransition phases. This rise in lateral forces also

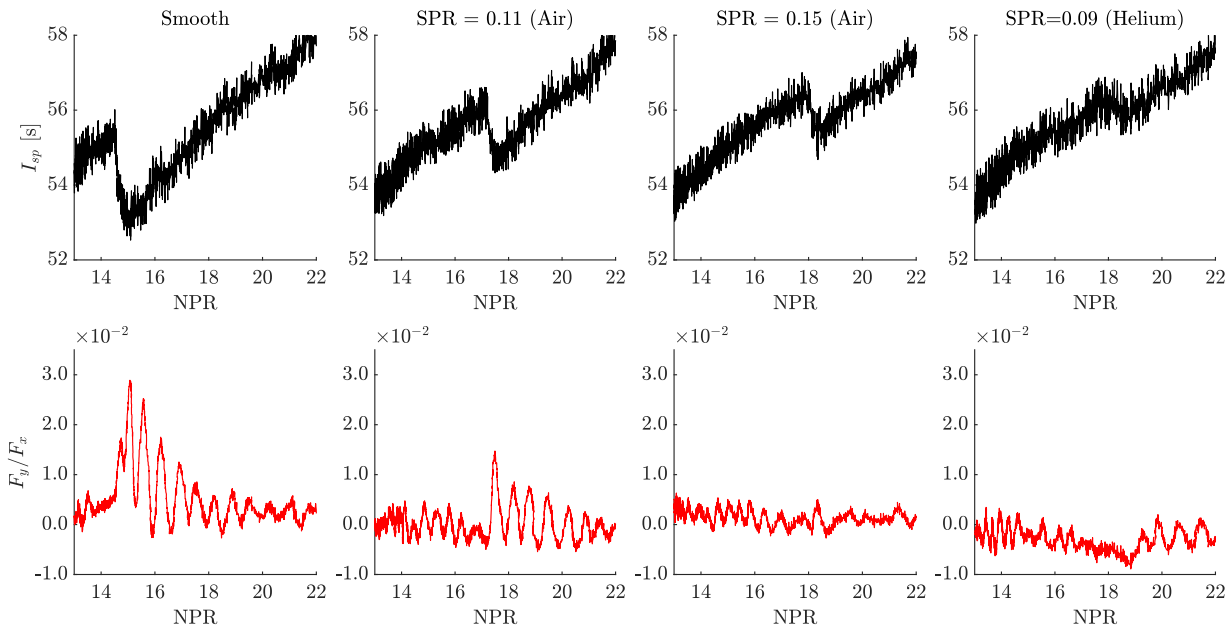

Figure 8: Instantaneous measurements of specific impulse (on top) and side-loads-to-thrust ratio (on bottom) during one transition phase for the smooth DBN, DBN with secondary injection of air and DBN with secondary injection of helium.

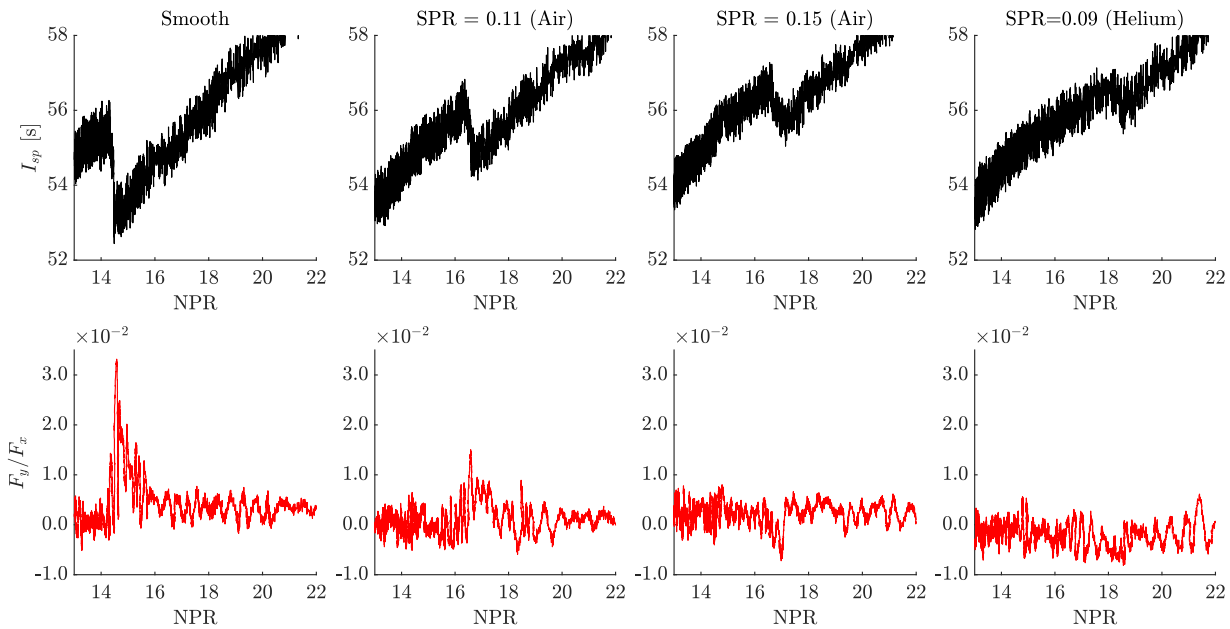

Figure 9: Instantaneous measurements of specific impulse (on top) and side-loads-to-thrust ratio (on bottom) during one retransition phase for the smooth DBN, DBN with secondary injection of air and DBN with secondary injection of helium.

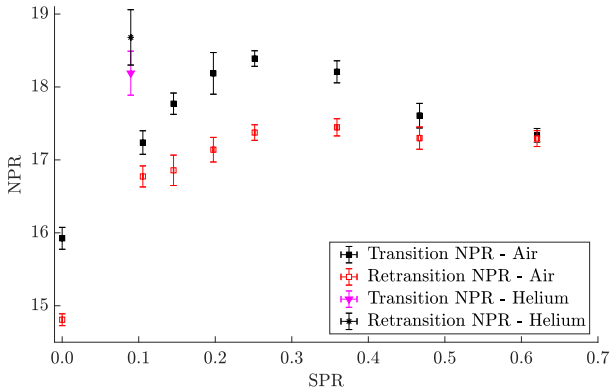

Figure 10: Transition and retransition NPR as a function of secondary pressure ratio. Error bars show the standard deviation calculated for each configuration.

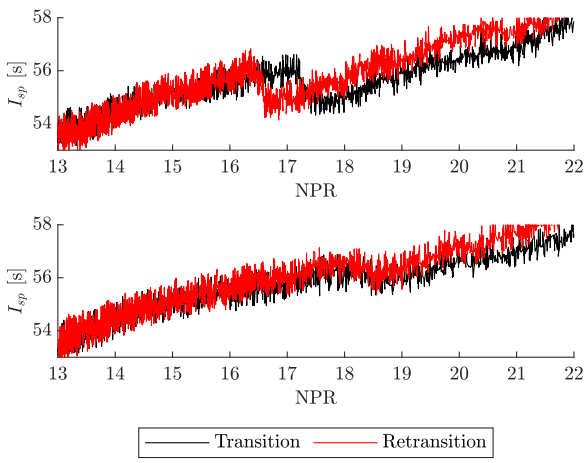

Figure 11: Specific impulse during a transition phase and a retransition phase as a function of NPR for secondary injection of air at SPR = 0.11 (top) and helium at SPR = 0.09 (bottom).

falls within the measurement noise.

The influence of secondary injection on thrust jump during the transitions and the retransitions is showed in Fig. 13. The test series revealed that the air SPR did not present any significant impact on the thrust jump magnitude during transition and retransition between SPR = 0.15 and SPR = 0.25 as it stays fairly constant, though much less important than in the smooth nozzle configuration, which showed 2.2 times higher values. For SPR = 0.11, the jumps magnitude during both, the ascent and the descent, are slightly higher than for the other cases. The latter observation might originate from the non-sonic secondary injection jet at SPR = 0.11 which can be a source of instability in the flow and a more thorough investigation is necessary to validate this hypothesis. Above SPR = 0.25, a further decrease in thrust jump is visible as

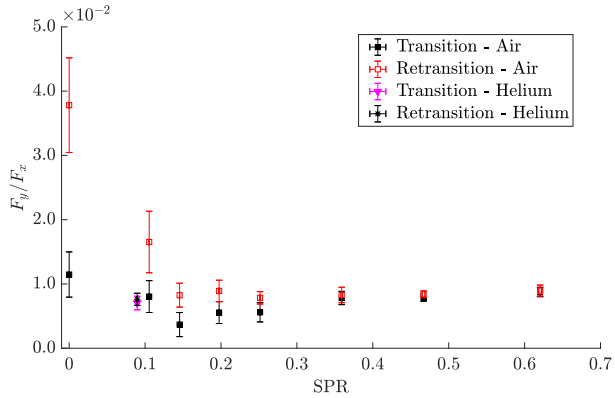

Figure 12: Side-loads-to-thrust ratio measured during transitions and retransitions as a function of secondary pressure ratio. Error bars show the standard deviation calculated for each configuration.

the secondary injection pressure is increased, though the maximum decrease remains fairly close to the values between SPR = 0.15 and SPR = 0.25. The maximum thrust jump decrease during transition using secondary injection of air led to 3.2 times lower values than measured in the smooth DBN configuration. Fig. 13 also reveals that no significant differences were measured between the SPR = 0 configuration and the different injection cases during transition. Nonetheless, the presence of air secondary injection reduced the thrust jump during retransition up to 67.6% compared to the SPR = 0 case, and 73.8% (a factor of 3.8) compared to the smooth nozzle configuration. The effect of helium secondary injection during transition and retransition was even more significant as the decrease in thrust jump compared to the smooth nozzle configuration exceeded 86% during the ascent and the descent phases. The significant error bars visible on Fig. 13 emanates from the difficulty to clearly identify the thrust jump magnitude in this configuration, especially because of the force balance measurements limitations.

4. CONCLUSIONS AND SUMMARY

This paper focused on comparing the impact of air and helium radial secondary injection on the DBN transition behaviour. Several air secondary pressure ratios (SPR) ranging from 0.11 to 0.62 were considered and one SPR for helium was used: 0.09. Compared to the smooth nozzle configuration (nozzle without secondary injection slot), the transition NPR was delayed at maximum by nearly 23.9% using an air SPR of 0.25, against an increase of 22.5% for a helium SPR of 0.09. Compared to the smooth nozzle configuration, the retransition NPR was increased at maximum by 20.1% for an air SPR of 0.36, against 28.6% for a helium SPR of 0.09. The several experiments using different air SPR showed that the

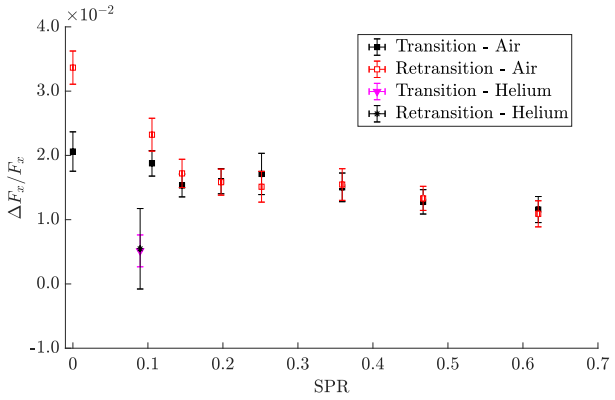

Figure 13: Thrust jump divided by the thrust during transitions and retransitions as a function of secondary pressure ratio. Error bars show the standard deviation calculated for each configuration.

transition and retransition NPR delay were limited. The side-loads were decreased below 1% of the nozzle thrust during the transition and the retransition phases using a secondary pressure ratio of air and helium of only 0.15 and 0.09, respectively. Moreover, secondary injection of air (resp. helium) reduced the thrust jump during transition up to 69.2% (resp. 86.3%) and during retransition up to 73.8% (resp. 86.8%) compared to the smooth nozzle configuration. A complete interpretation of the present results necessitates further numerical work and a parametrical investigation of the helium secondary injection will be an interesting aspect of DBNs regime transition control. Nonetheless, the previous results would be extremely suitable should dual-bell nozzles with secondary injection be used in any current or next generation of launchers.

5. ACKNOWLEDGMENT

We would like to gratefully acknowledge the laboratory of Excellence CAPRYSSES framework and the financial support of this study from Grant No. ANR-11-LABX-0006-01 of the Investissements d'Avenir LabEx CAPRYSSES. We would also like to thank Nicolas Gouillon for his technical assistance.

REFERENCES

[1] Ralf Stark, Chloé Génin, Dirk Schneider, and Christian Fromm. Ariane 5 performance optimization using dual-bell nozzle extension. *Journal of Spacecraft and Rockets*, 53:743–750, 2016.

[2] Swan Walter .C. The influence of nozzle design on the flight performance of rocket vehicles, with an analysis of the results of jet separation, 1948.

[3] Manuel Frey and Gerald Hagemann. Critical assessment of dual-bell nozzles. *Journal of Propulsion and Power*, 15:137–143, 1999.

[4] Gerald Hagemann, Michael Terhardt, Dietrich Haeseler, and Manuel Frey. Experimental and analytical design verification of the dual-bell concept. *Journal of Propulsion and Power*, 18:116–122, 2002.

[5] K Kusaka, A Kumakawa, M Niino, A Konno, and M Atsumi. Experimental study on extendible and dual-bell nozzles under high altitude conditions. 2000.

[6] G. E. Dumnov, N. B. Ponomaryov, and A. L. Voinov. Dual bell nozzles for rocket engines of launch vehicle upper stages and orbital transfer vehicles. American Institute of Aeronautics and Astronautics Inc, AIAA, 1997.

[7] Andrea Ferrero, Antonietta Conte, Emanuele Martelli, Francesco Nasuti, and Dario Pastrone. Dual-bell nozzle with fluidic control of transition for space launchers. *Acta Astronautica*, 193:130–137, 4 2022.

[8] Chloe Nürnberger-Genin and Ralf Stark. Flow transition in dual bell nozzles. *Shock Waves*, 19:265–270, 7 2009.

[9] Chloé Génin and Ralf H. Stark. Side loads in subscale dual bell nozzles. *Journal of Propulsion and Power*, 27:828–837, 2011.

[10] S. B. Verma, R. Stark, and O. Haidn. Gas density effects on dual-bell transition behavior. *Journal of Propulsion and Power*, 28:1315–1323, 2012.

[11] Vladeta Zmijanovic, Luc Leger, Mohamed Sellam, and Amer Chpoun. Assessment of transition regimes in a dual-bell nozzle and possibility of active fluidic control. *Aerospace Science and Technology*, 82-83:1–8, 11 2018.

[12] Chloé Génin and Ralf Stark. Experimental investigation of the inflection geometry on dual bell nozzle flow behavior. 2011.

[13] Chloé Génin, Andreas Gernoth, and Ralf Stark. Experimental and numerical study of heat flux in dual bell nozzles. *Journal of Propulsion and Power*, 29:21–26, 2013.

[14] Francesco Nasuti, Marcello Onofri, and Emanuele Martelli. Role of wall shape on the transition in axisymmetric dual-bell nozzles. *Journal of Propulsion and Power*, 21:243–250, 2005.

[15] Takeo Tomita, Mamoru Takahashi, Masaki Sasaki, and Hiroshi Tamura. Investigation on characteristics of conventional-nozzle-based altitude compensating nozzles by cold-flow tests. 2006.

[16] Francesco Nasuti, Marcello Onofri, and Emanuele Martelli. Numerical study of transition between the two operating modes of dual-bell nozzles. 2002.

[17] M Horn and S Fisher. Dual-bell altitude compensating nozzles, 1993.

[18] S. B. Verma, R. Stark, and O. Haidn. Reynolds number influence on dual-bell transition phenomena. *Journal of Propulsion and Power*, 29:602–609, 2013.

[19] Emanuele Martelli, Francesco Nasuti, and Marcello Onofri. Numerical parametric analysis of dual-bell nozzle flows. *AIAA Journal*, 45:640–650, 3 2007.

[20] R. Stark and C. Génin. Flow separation in rocket nozzles under high altitude condition. *Shock Waves*, 27:63–68, 1 2016.

[21] Vladeta Zmijanovic, Luc Leger, Eric Depussay, Mohamed Sellam, and Amer Chpoun. Experimental-numerical parametric investigation of a rocket nozzle secondary injection thrust vectoring. *Journal of Propulsion and Power*, 32:196–213, 2016.

[22] Ralf H. Stark and Chloé Génin. Experimental study on rocket nozzle side load reduction. *Journal of Propulsion and Power*, 28:307–311, 2012.

[23] Dirk Schneider, Ralf Stark, Chloé Génin, Michael Oschwald, and Konstantin Kostyrkin. Active control of dual-bell nozzle operation mode transition by film cooling and mixture ratio variation. *Journal of Propulsion and Power*, 36:47–58, 2019.

[24] Dzianis Proshchanka, Koichi Yonezawa, Hidekazu Koga, Yoshinobu Tsujimoto, Tatsuya Kimura, and Kazuhiko Yokota. Control of operation mode transition in dual-bell nozzles with film cooling. *Journal of Propulsion and Power*, 28:517–529, 2012.

[25] Emanuele Martelli, Francesco Nasuti, and Marcello Onofri. Numerical analysis of film cooling in advanced rocket nozzles. *AIAA Journal*, 47:2558–2566, 11 2009.

[26] L. Léger, V. Zmijanovic, M. Sellam, and A. Chpoun. Controlled flow regime transition in a dual bell nozzle by secondary radial injection. *Experiments in Fluids*, 61, 12 2020.

[27] L. Léger, V. Zmijanovic, M. Sellam, and A. Chpoun. Experimental investigation of forced flow regime transition in a dual bell nozzle by secondary fluidic injection. *International Journal of Heat and Fluid Flow*, 89, 6 2021.